Epoxidised Natural Rubber (ENR)/Wollastonite Composites for Tyre Inner Liners: A Practical Replacement for Butyl Rubber in Industrial Applications

ÜNÜGÜL YAVUZ, Tuba, ESSA, Abdusalam, JANANI, Ronak, KARAAĞAÇ, Bağdagül and SAMMON, Chris <http://orcid.org/0000-0003-1714-1726>

Polymer Engineering & Science

WILEY | spe INSPIRING PLASTICS PROFESSIONALS

RESEARCH ARTICLE OPEN ACCESS

Epoxidised Natural Rubber (ENR)/Wollastonite Composites for Tyre Inner Liners: A Practical Replacement for Butyl Rubber in Industrial Applications

Tuba Ünügül Yavuz[1,2] | Abdussalam Essa[3] | Ronak Janani[3] | Bağdagül Karaağaç[1,3] | Christopher Sammon[3]

[1]Department of Chemical Engineering, Kocaeli University, Umuttepe Campus, Kocaeli, Turkey | [2]Özka Tyre, Kocaeli, Turkey | [3]School of Engineering and Built Environment, Sheffield Hallam University, Sheffield, UK

Correspondence: Bağdagül Karaağaç (bkaraagac@kocaeli.edu.tr)

Received: 15 September 2025 | **Revised:** 12 November 2025 | **Accepted:** 14 November 2025

Keywords: adhesion | butyl rubber | epoxidised natural rubber | gas barrier properties | tyre inner liner compound | wollastonite

ABSTRACT

This study aimed to develop epoxidised natural rubber (ENR)-based rubber compound formulations as an alternative to butyl rubber for tyre inner liners. The effects of different vulcanization systems, designed to achieve similar curing behavior in NR-based carcass compounds and ENR-based liner compounds, were evaluated. The selected vulcanization system was applied to other compound formulations in subsequent stages to enhance adhesion and gas barrier properties. The impact of high-aspect-ratio wollastonite on interfacial adhesion was evaluated for the first time in an ENR matrix. Additionally, the effects of varying wollastonite concentrations on the adhesion and gas barrier properties of the liner compound were examined. The compounds were assessed based on their rheological, physical, and mechanical properties, adhesion strength, gas permeability, and topographical characteristics. It was concluded that the coagent-induced vulcanization system was the most effective for co-vulcanization of NR and ENR. Additionally, adhesion and gas barrier properties were significantly enhanced by incorporating relatively low amount (5 phr) of wollastonite into ENR without notable changes in mechanical properties. The proposed formulation demonstrated adhesion between the carcass and liner compound that is approximately eight times higher than existing butyl liner applications while achieving lower gas permeability than butyl rubber.

1 | Introduction

The tyre can be considered an elastic composite material, which maintains air at a certain pressure and provides contact between the road and the vehicle. It consists of several different rubber layers to meet various performance demands. It is extremely important that composition of these compounds is designed such that simultaneous vulcanization at optimum level is achieved for better tyre integrity and durability. Among these rubber compounds, the inner liner compound is the most challenging to design due to its very distinct curing characteristics. The liner consists of a rubber matrix with low gas permeability so that it can encapsulate high-pressure air inside the tyre. Enhancing the vulcanization process of the liner compound alongside the carcass, which is the structural framework of the tyre, consisting of layers of fabric cords that provide strength and flexibility, is crucial for overall tyre performance, particularly its dynamic behavior at high speeds and accelerations. For the tyre inner liner to exhibit good gas barrier properties and long service life, only a limited number of specific rubbers can be used in their production [1]. The majority of tyre manufacturers prefer to utilize halogenated butyl rubber (bromobutyl (BIIR) or chlorobutyl (CIIR) rubber) for liners due to their superior gas barrier performance [2–4]. However, butyl rubbers have some shortcomings such as incompatibility with other rubber compounds used in the tyre structure due to their

Highlights

- ENR compounds for tyre inner liners with superior adhesion & barrier properties.
- Optimized coagent-induced vulcanization for NR/ENR.
- First study on high-aspect-ratio wollastonite boosting ENR matrix adhesion.
- 5 phr amino silane wollastonite gave superior adhesion & lower gas permeability.
- Formulation beat butyl rubber in adhesion & barrier without mechanical loss.

different unsaturation level and inherently poor mechanical properties [5–7].

Although improved mechanical properties can be achieved by using natural rubber and certain synthetic rubbers, their use in liner compounds is limited due to their relatively high gas permeability. In recent years, an increasing number of attempts have been made to use epoxidised natural rubber (ENR) in lining applications due to its desirable gas barrier properties and good mechanical performance [1, 8–9]. ENR, a new generation semi-natural rubber, exhibits relatively high polarity due to random arrangement of epoxy groups on the polymer backbone, and so it is considered promising for replacing nitrile rubber (NBR) for applications requiring good resistance to oils and hydrocarbon-based liquids [10, 11]. In addition, since it has improved wet grip, high adhesion and damping properties, ENR can be used in the production of high-performance industrial materials with, or in place of, natural rubber and common synthetic rubbers (e.g., styrene-butadiene rubber (SBR)) [12, 13].

ENR is produced by chemical modification of natural rubber with formic peroxy acid and is commercially available with various epoxy content. The most widely used grades are ENR-50 and ENR-25, which contain 50% and 25% (mol%) epoxy groups on the main chain, respectively [14]. Due to its relatively high polarity, ENR can be used as a compatibiliser to improve the dispersion of polar fillers such as silica in non-polar rubber matrices [15–18]. The potential of using ENR as an alternative to butyl rubber for various applications has been cited in the literature [1, 8–9]. Sankaran et al. [8] studied the effect of ENR on the properties of BIIR/ENR-50 (75/25) blends prepared with nano-clay (Cloisite 20). They reported that the tensile strength and tear resistance of the vulcanizates increased with increasing Cloisite 20 concentration due to the reinforcing effect of the nano-clay. The best interphase and the lowest gas permeability were obtained with 3 phr nano-clay addition. Raju et al. [1] investigated the effect of graphene nanoplate (GNP) at different ratios (0–6 phr) to halogenated butyl rubber and ENR (ENR-25 and ENR-50) blends on the mechanical and barrier properties of inner liner compounds. Since the presence of epoxy groups is responsible for preventing gas permeation, better barrier properties were obtained for BIIR/ENR-50 blends. Aswathy et al. [9] studied rheological, mechanical, and thermal properties of 4 phr graphene oxide, Laponite® or nano-silica containing BIIR/ENR-50 (75/25) compounds along with their gas barrier properties. Approximately 20% increase in mechanical strength and 15% decrease in gas permeability were obtained for all nanofiller additions. This was attributed to nanofillers not only reinforcing the rubber matrix but also exhibiting a barrier effect by making the gas diffusion pathway more tortuous.

Fillers are also of great importance in improving interphase adhesion and reducing gas permeability by inhibiting molecular movement in the material structure. However, in order to achieve this property from fillers, it is important for them to have sufficient compatibility with the rubber to be able to disperse effectively within the rubber matrix [19, 20]. Fillers are classified as layered (such as bentonite, montmorillonite, graphene nanoplate), porous (such as clinoptilolite, zeolite), tubed (carbon nanotube, halloysite nanotube), and rod-like (such as wollastonite, sepiolite) according to their structures. The impact of fillers on the polymeric matrix is directly related to their structures. High aspect-ratio (rod-like) fillers, can improve mechanical strength of the rubber as well as increase the adhesion between polymer layers, especially when oriented perpendicular to the surface. Wollastonite is a bright white natural calcium metasilicate composed of calcium, silicon, and oxygen and is preferred as a functional filler due to its rod-like structure [21, 22]. In order to increase the reinforcing effect of wollastonite and to ensure a homogeneous dispersion in the rubber compound, its surface can be modified with reactive silanes such as amino, epoxy, methacryl, methyl, trimethyl and vinyl functional silanes [23]. Commercial silane-modified wollastonite grades are widely available on the market. There are many studies in the literature in which the final product properties are improved by adding wollastonite to rubber compounds [24–29]. Diep et al. [25] investigated the rheological, mechanical and topographical properties of the compounds prepared by adding 10–40 phr wollastonite to natural rubber and showed that vulcanization occurred faster with an increase in the amount of wollastonite. However, this came with the penalty of a modest decrease in the tensile strength and elongation at break. Chatterjee et al. [30] investigated the effects of neat wollastonite and vinyl silane-modified wollastonite on the properties of SBR-based rubber compounds. They observed that vinyl silane modification provided strong interaction with SBR due to the presence of active functional groups on the wollastonite surface resulting in improved mechanical strength. The addition of 3% modified wollastonite significantly improved the thermal stability of the vulcanizates due to its excellent dispersion. Akçakale and Bülbül [31] investigated the effect of various amounts of mica powder and wollastonite on the physical and mechanical properties of NR/SBR blends. They reported that increasing the concentration of wollastonite and mica powder led to higher hardness and abrasion resistance, while a moderate decrease in tensile strength, elongation at break, and fatigue resistance was observed. Xiao et al. [28] investigated the effect of adding silica and wollastonite to NR (at different ratios: 60/0, 40/20, 20/40, 0/60 phr), on the rheological, mechanical, and dynamic-mechanical properties. They reported that wollastonite can improve the compatibility between silica and natural rubber resulting in better processability and higher mechanical strength.

Along with the main polymer matrix and reinforcing/functional fillers, rubber compounds consist of several key components

that work together to achieve desired mechanical and thermal properties. Mineral oils, such as naphthenic oil, act as a plasticizer, enhancing processability and flexibility. Vulcanization activators, typically zinc oxide and stearic acid, promote efficient crosslink formation during curing. Stabilizers, including antioxidants and antiozonants, protect the rubber from oxidative and ozone-induced degradation, extending its service life. Phenolic resins function as a reinforcing resin, enhancing hardness, adhesion, and heat resistance. Vulcanization accelerators control the rate and efficiency of crosslinking reactions, and sulfur serves as the primary vulcanising agent, forming crosslinks between rubber chains to improve elasticity and overall mechanical strength [32, 33].

This study aimed to develop an epoxidised natural rubber-based compound as an alternative to butyl rubber-based tyre inner liner compounds, with good gas barrier properties and improved adhesion to the other tyre rubber compounds. Wollastonite, which is a natural mineral filler with high aspect ratio, was incorporated to ENR in order to achieve desired adhesion and barrier properties along with good mechanical performance.

2 | Materials and Methods

2.1 | Materials

Natural rubber (SIR 10) was supplied from Indonesia with 60 ± 5 MU of Mooney viscosity (ML (1 + 4)@100°C) and 82 of plasticity retention index. Bromo butyl rubber (BIIR) was purchased from Exxon-Mobile with 32 ± 4 MU of Mooney viscosity (ML (1 + 8)@125°C) and 1.9% of bromine content. Epoxidised natural rubber (Epoxyprene-50) with 50% (mol%) epoxy content was purchased from Muang Mai Guthrie Public Company Ltd. with 80 ± 5 MU of Mooney viscosity (ML (1 + 8)@100°C). HAF N330 carbon black obtained from OMSK (Russia) was used as reinforcing filler. Amino silane-modified wollastonite (Elminax Fillex AF-1) with an aspect ratio of 1:15 was supplied from Elminas Mineral, Turkey. Naphthenic oil (Octopus NW 922) was obtained Petroyağ (Turkey) with 0.906 g/cm^3 of density and 104 cSt of viscosity (@40°C). N, N′-m-phenylene bismaleimide (HVA-2) was supplied from Resinex, Turkey. Phenolic resin (SP 1068, pure phenolic with an acid number of 0–35 and 68°C–78°C of softening point) was obtained from SI Group, Bethune. Zinc oxide (325 μm) was purchased from Metal Oxide, Turkey. Stearic acid (softening point 52°C–62°C), 2,2,4-trimethyl-1,2-dihydroquinoline (TMQ), *N*-isopropyl-*N*′-phenyl-*p*-phenylenediamine (IPPD), ozone wax, and cure system components CBS (*N*-cyclohexyl benzo thiazole sulphenamide), DCBS (benzothiazyl-2-dicyclohexyl sulphenamide), DPTT (di-pentamethylene thiuram tetrasulfide), MBT (2-mercaptobenzothiazole), TBzTD (tetrabenzyl thiuram disulfide), TMTD (tetramethyl thiuram disulfide) and sulfur were all purchased from Zeta Rubber, Turkey.

2.2 | Methods

Rubber compounds were prepared by using a 2 L (gross volume) internal mixer (Met-Gür, Turkey) and then sheeted out on a laboratory mill. ENR was masticated first, for 2 min at a rotor speed of 30 rpm to obtain desired flow properties. Carbon black, wollastonite, and process oil were then fed into the mixer and mixed for 1 min at 25 rpm. In the next three steps, a 30 s interval was applied between activators (zinc oxide and stearic acid), stabilizers (TMQ and 6PPD), and the cure system. The final compound was then mixed for 1 min further and dumped from the mixer at approximately 60°C. A 150 mm wide laboratory-type two-roll mill with a friction ratio of 1:1.1 was used for the final homogenization and shaping of the compound. Rubber compound preparation methodology has been summarized in Figure 1.

A generic natural rubber-based carcass compound (NR), which is in direct contact with the tyre inner liner compound during tyre curing process, was prepared as an adhesion base to evaluate the adhesion performance of the ENR compounds. Another generic BIIR based tyre inner liner compound (REF) was also prepared as reference. Sample groupings and classification is summarized in Figure 1, and all compound formulations are given in Table 1. ENR compounds are evaluated in two separate groups. The first group consists of three ENR compounds, which have different cure packages to select the best cure system for similar cure behavior to the NR base compound in order to obtain desired adhesion between the liner and the carcass. CV, EV, and HV compounds were prepared by using conventional, efficient, and bismaleimide-induced curing systems, respectively. The second group of compounds (Table 1) were prepared using various amounts of wollastonite to evaluate the effect of wollastonite concentration, particularly on the gas barrier properties. In this group, the cure package was based on a bismaleimide-induced system (HV), and the compound codes refer to the amount of wollastonite used in the compound.

Alpha Technologies RPA 2000 rubber process analyzer (RPA) was used to measure the optimum cure times of the rubber compounds according to ASTM D5289. Compounds were then vulcanized on a hydraulic hot press under 150 bar pressure and for their respective cure times (time corresponding to maximum torque) at 150°C.

Dynamic strain sweep tests were performed by using RPA to evaluate the Payne effect for uncured samples according to ASTM D8059. Storage modulus (G') values were recorded for 0.5%–200% strain range at 0.3 Hz and at 100°C. A frequency sweep test was also performed on the RPA to examine the processability. Before starting the test, the compound samples were conditioned at 100°C for 1 min. While the compound samples were still in the mold, the damping factor (tan δ) was measured in the frequency range of 0.01–33 Hz at 100°C and at 7% strain level.

Mechanical properties of Die C dumb-bell shaped vulcanizates were measured by using a universal testing machine (Zwick Roell Z010) with 500 mm/min crosshead speed according to ASTM D412. Hardness measurements were carried out on cylindrical samples in 6 mm thickness using a Zwick Roell durometer according to ASTM D2240. Vulcanizates were subjected to thermal aging in an air circulating oven for 70 h at 100°C fixed temperature, in accordance with ASTM D573. Physical and

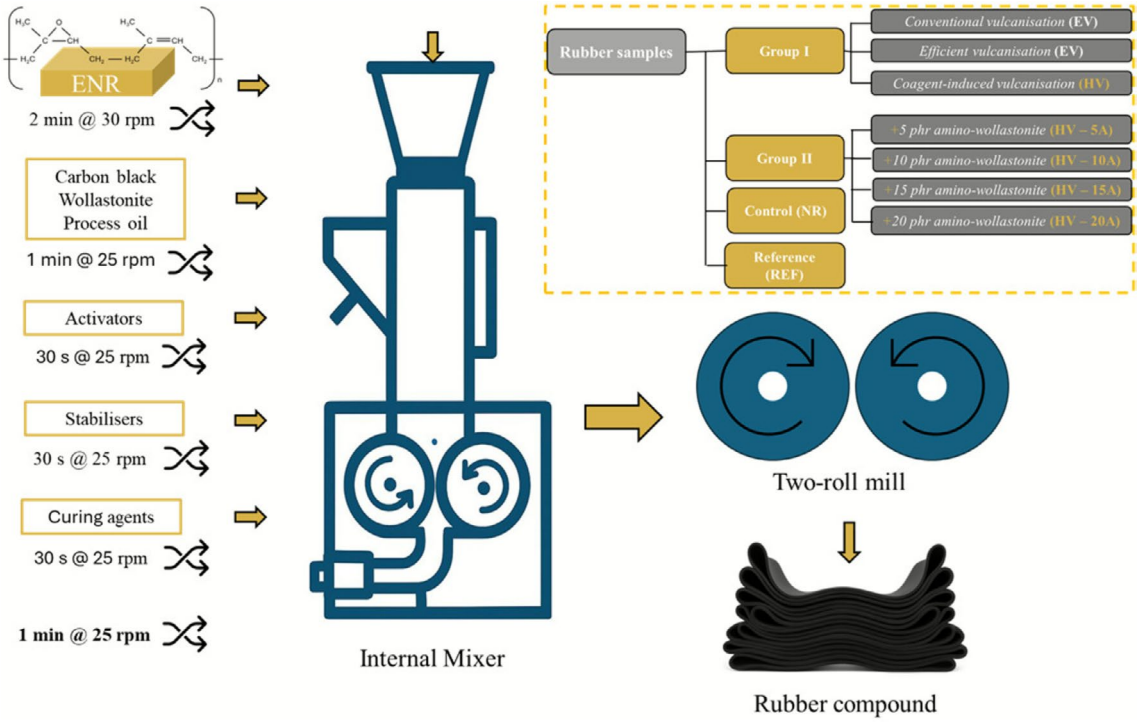

FIGURE 1 | Rubber compound preparation methodology.

TABLE 1 | Rubber compound formulations.

	NR	REF	CV	EV	HV	HV-5A	HV-10A	HV-15A	HV-20A
	Content (phr)								
NR	100	—	—	—	—	—	—	—	—
BIIR	—	100	—	—	—	—	—	—	—
ENR-50	—	—	100	100	100	100	100	100	100
N330	40	40	40	40	40	40	40	40	40
Silica	10	—	—	—	—	—	—	—	—
Wollastonite	—	—	—	—	—	5	10	15	20
Naphthenic oil	10	—	10	10	10	10	10	10	10
Castor oil	—	5	—	—	—	—	—	—	—
Activators	7	5	7	7	7	7	7	7	7
Stabilizers	2	—	2	2	2	2	2	2	2
Phenolic resin	4	—	—	—	—	—	—	—	—
Accelerators	2	2.5	1.5	4.0	2.0	2.0	2.0	2.0	2.0
HVA-2	—	—	—	—	3.0	3.0	3.0	3.0	3.0
Sulfur	3	2	2.5	1.0	1.0	1.0	1.0	1.0	1.0

mechanical tests were also performed after thermal aging and the retention in the properties were reported.

Adhesion between the inner liner compounds and NR base compound was characterized with T-peel test according to ASTM D1876. In this method, the two different compound samples, both of 1 mm thickness, are placed in contact, while one end of the samples are separated with a polyester film to obtain sufficient length to attach the jaws of the tensile tester. T-peel test samples are then vulcanized in a 2 mm thickness mold for the optimum cure times of two compounds. After conditioning, the samples are subjected to tensile deformation with a crosshead

speed of 125 mm/min, and the average results of five replicates were reported as adhesion force in N. The T-peel adhesion test procedure is depicted in Figure 2.

The determination of gas permeability was carried out according to ASTM D1434-82, by employing the setup at room temperature. Permeability factor (P), which is inversely proportional to gas barrier properties, was calculated as a function of diffusivity (D) and solubility (S) as expressed in Equation (1), where Q is the volumetric flow rate of the gas (cm^3/s), Δp is the applied pressure to the membrane (cm Hg), A is the effective membrane area (cm^2), and l is the thickness of the membrane in cm.

$$P = DS = \frac{Ql}{\Delta pA} \tag{1}$$

Permeability values are expressed in Barrer (1 Barrer = 10^{-10} cm^3 (STP) cm/(cm^2s cmHg)) [34]. Figure 3 shows the gas permeability test setup used in the study. This setup mainly consists of a stainless-steel membrane cell, pressure controller, and digital flow meter [35–37]. The pressure gradient was generated by pressurized feed gas (planned flow rate 40 cm^3/min) with an effective separation area of 7 cm^2. The gas separation tests were then carried out at 25°C, 2 bar and 4 bar in order to investigate the barrier properties at the target pressure as well as the at the limit pressure conditions. Note that the air pressure in automobile tyres is typically 38–40 psi (2.6–2.75 bar). Gas permeability measurements continued until the permeability reached steady state and the measurements were repeated three times for each vulcanized sample.

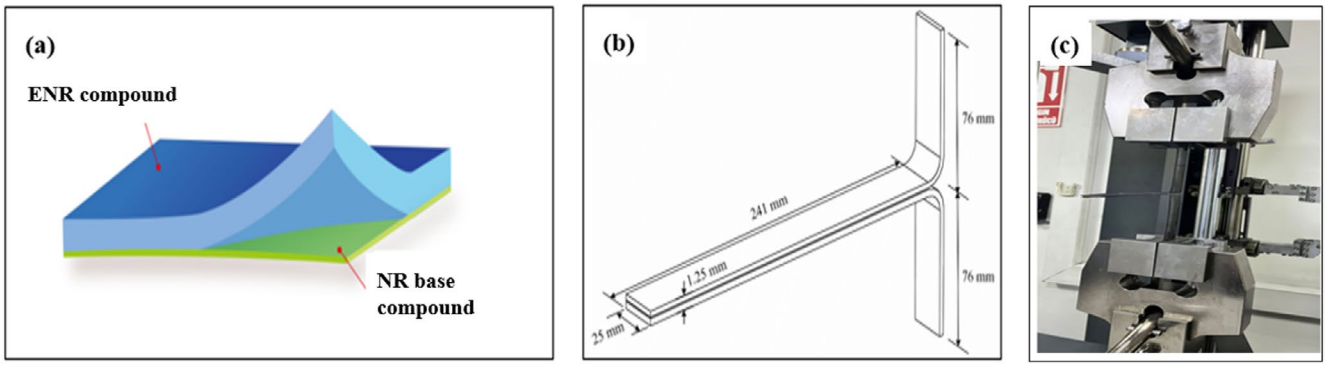

FIGURE 2 | Schematic representation of T-peel adhesion test.

FIGURE 3 | Gas permeability test setup.

All samples were cut into two pieces in order to scan the cross-sectional view for each sample. Samples were then mounted onto aluminum stubs and gold coated using (Q150T-ES sputter coater Quorum, UK) (10lA sputter current for 190 s with a 2.7 tooling factor). Scanning electron microscopy (FEI NOVA nano SEM 200), was used to capture images of rubber samples in low vacuum mode, with an operational water vapor pressure of 0.8–1 Torr, accelerating voltage of 5–7 kV and magnification ranged between 100 and 20,000×.

3 | Results and Discussion

In this study, ENR compounds were separated into two different groups. The first group of compounds (Group-1) was prepared with different cure packages to identify the optimal cure system for achieving curing behavior analogous to the NR-based compound. The second group of compounds (Group-2) contained amino silane-modified wollastonite in various amounts. They were characterized in order to understand the effect of wollastonite, particularly on the gas barrier properties of ENR-based inner liner compounds.

3.1 | Selecting the Cure System

To optimize interfacial adhesion by achieving similar curing behavior and cure rates, compounds were formulated using three distinct vulcanization systems: conventional (CV), efficient (EV), and coagent-induced (HV). Rheological, mechanical and adhesion properties were measured and compared with a generic butyl compound (REF). Cure curves of Group-1 compounds obtained at 150°C are given in Figure 4. Minimum torque (ML) indicating the compound viscosity, maximum torque value showing the final stiffness, scorch time (t_{s2}), which refers the period before rapid vulcanization begins, and optimum cure time (t_{90}), which is the time required to reach 90% of the maximum cure, were calculated from the cure curves and given in Table 2. Cure extent (CE) and cure rate index (CRI) were calculated according to Equations (2) and (3), respectively and are also provided in Table 2. CE represents the degree of vulcanization achieved relative to the maximum torque, while the CRI indicates the speed of vulcanization, calculated from the inverse of the time difference between scorch time and t_{90}.

$$\text{Cure extent} = \text{MH} - \text{ML} \tag{2}$$

$$\text{Cure rate index} = 100 / \left(t_{90} - t_{s2}\right) \tag{3}$$

NR and REF compounds have very distinct cure profiles from each other (Figure 4 and Table 2); therefore, poor adhesion is expected between these two compounds. Comparison of rheological properties indicates the most noticeable difference between the compounds is their vulcanization rate followed by their cure extent. Since the REF sample is based on butyl rubber, it is expected to exhibit a significantly different behavior in both aspects. It was observed that ENR compounds are cured at a rate very similar to NR in CV, while curing at a relatively lower rate in other systems. In all these compounds, a higher cure extent, i.e., a greater degree of crosslinking, was achieved compared to

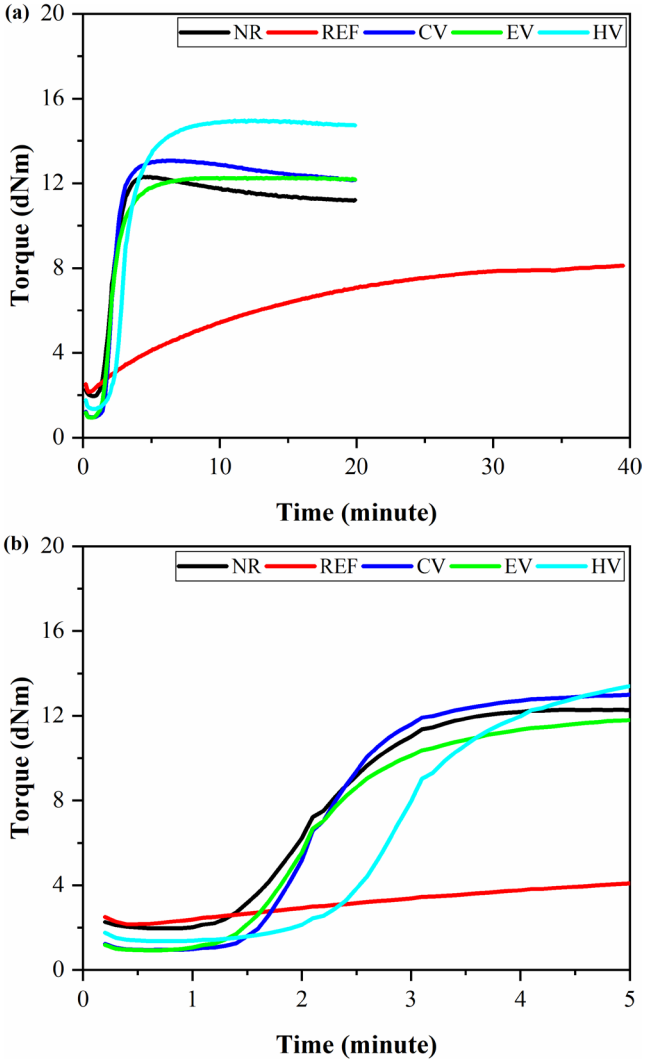

FIGURE 4 | Effect of cure system: (a) Rheometer curves, (b) Extended rheometer curves of the Group-1 compounds.

both NR and REF compounds. This is attributed to the epoxy functionality on the ENR main chain participating in the vulcanization reaction, leading to additional chemical interactions [38–40]. Furthermore, the relatively low Mooney viscosity has been considered a favorable factor, as it facilitates the processing of the tyre inner liner compound in the final shaping equipment such as extruders and calendrers.

One of the key properties in inner liner compounds is scorch safety. Indeed, since liner compounds are produced at relatively low thickness and go through multiple processing steps before reaching their final form, it is crucial that they do not begin to cure prematurely. When butyl rubber is used, this issue can be easily resolved [1]. However, when an alternative rubber matrix is used instead of butyl rubber, especially a rubber matrix containing an isoprene structure, scorch safety becomes a critical concern. In this context, scorch safety can be considered one of the most important criteria in selecting an appropriate curing system for the compounds. Based on the ts_2 values recorded in Table 2, the butyl rubber-based REF sample has a distinct level of scorch time compared to the other systems. Among all systems, the HV sample demonstrated the closest scorch time to that of the REF sample, where vulcanization was carried out in the presence of a coagent.

TABLE 2 | Rheological data of the Group-1 compounds.

	ML (dNm)	MH (dNm)	t_{s2} (min)	t_{90} (min)	CE (dNm)	CRI (min^{-1})
NR	2.8 ± 0.1	12.9 ± 0.2	1.7 ± 0.1	3.2 ± 0.1	10.2 ± 0.2	64.6 ± 2.4
REF	2.2 ± 0.1	8.2 ± 0.1	4.3 ± 0.1	25.8 ± 0.1	6.1 ± 0.1	4.7 ± 0.1
CV	1.4 ± 0.1	14.4 ± 0.3	1.7 ± 0.1	3.1 ± 0.1	12.9 ± 0.3	68.2 ± 1.0
EV	1.4 ± 0.1	13.3 ± 0.2	1.5 ± 0.1	3.6 ± 0.1	11.9 ± 0.2	47.8 ± 1.8
HV	1.3 ± 0.1	15.0 ± 0.1	2.3 ± 0.1	5.2 ± 0.1	13.7 ± 0.1	34.3 ± 1.1

Physical and mechanical properties of the vulcanizates were measured both for initial samples and for the samples subjected to thermal aging at 70°C for 70 h. Figure 6a–d highlight the results for tensile strength, elongation at break, 100% tensile modulus, and hardness, respectively. It was observed that the mechanical properties of all ENR-based vulcanizates were approximately 2 times higher than those of the REF compound. This was expected as the mechanical strength of ENR is inherently superior to that of butyl rubber. At the same time, the mechanical properties of NR- and ENR-based samples were similar. This is a very promising finding for tyre applications. One would anticipate that the interface will be more compatible after the co-vulcanization of rubber layers with similar mechanical strength. When the mechanical properties of the compounds prepared using different vulcanization systems were examined, it was concluded that the best properties were obtained in the EV compound. In the literature, numerous studies show that vulcanizates prepared with the CV vulcanization system exhibit better mechanical properties compared to those prepared with the EV system. This is mainly due to the dominance of poly- and di-sulfide crosslinks (accounting for approximately 95% of all crosslinks) over mono-sulfide crosslinks (approximately 5% of all crosslinks) in the CV system [41–44]. However, this distinct difference between vulcanization systems is valid for rubbers with high unsaturation, such as NR, SBR, and BR. Since the crosslinking mechanism of ENR occurs not only through sulfur vulcanization but also via reactive epoxy groups, it exhibits a different behavior from conventional systems. It has been observed that ENR vulcanizates prepared with semi-EV and EV vulcanization systems have better mechanical properties compared to those prepared with the CV system [45–47].

When evaluating the effects of thermal aging on mechanical properties (Figure 5), it is noteworthy that vulcanizates prepared with the coagent (HVA-2) system exhibited less retention in mechanical properties after aging. This effect can be attributed to the ability of HVA-2 to form additional stable crosslinks between rubber chains, which has been considered a significant advantage. During thermal aging, oxidation and chain scission reactions typically lead to a reduction in tensile strength and elongation due to network degradation and embrittlement of the rubber matrix. However, the presence of HVA-2 appears to mitigate these effects by enhancing the crosslink stability, preventing the reversion, and so maintaining a more robust network structure. This stabilization effect results in a smaller decrease in mechanical performance compared to conventional systems, confirming the protective role of coagents under oxidative and thermal stress, which is highly desirable for long-term applications such as tyre inner liners.

The adhesion performance of the compounds in Group-1 to a NR-based compound surface was evaluated. It was observed that the butyl-based REF compound provides the lowest adhesion strength to the NR base (Figure 6). This difference can be attributed to the significantly varying levels of unsaturation between natural rubber and butyl rubber, which was an expected outcome. Adhesion strength of all ENR-based compounds was determined to be at least 5 times higher than that of the REF compound. The substantial improvement in adhesion can be attributed to the similar chemical structures of NR and ENR, the smaller difference in their unsaturation levels compared to butyl rubber, and ENR's ability to undergo additional chemical interactions beyond sulfur crosslinking, thanks to its reactive structure. As shown in Figure 4, the vulcanization system, along with the rubber matrix, also affects adhesion. When comparing the efficiency of the vulcanization systems, it was observed that compounds prepared with the CV and EV systems exhibited slightly higher adhesion strength than those prepared with the coagent-induced vulcanization system (HV). This can be attributed to the fact that, the curing profiles of these compounds are more like NR (as shown in Figure 4). However, despite the slightly lower adhesion strength compared to the CV and EV compounds, the HV system was deemed suitable as the base formulation for evaluating the effect of wollastonite addition in the Group-2 compounds. This decision was based on the significantly smaller changes in mechanical properties after aging, the almost identical tensile modulus values before aging, and the considerable improvement in scorch safety. Indeed, in industrial tyre inner liner applications, the compound is exposed to high temperature during the molding step, which requires the compound to be as resistant as possible to premature curing. Additionally, it is known that there is a less reduction in mechanical properties during thermal aging positively impacts the service life of the rubber product.

3.2 | Impact of Wollastonite on ENR-Based Rubber Compounds

In this study, ENR-based compounds (Group-2) were prepared with amino silane-modified wollastonite (with a 1:15 aspect ratio) in varying amounts (5–20 phr) and compared with the carcass compound (NR base compound) and a generic butyl rubber compound (REF) used in tyre inner liner applications. Rheological, mechanical, adhesion, and gas barrier properties

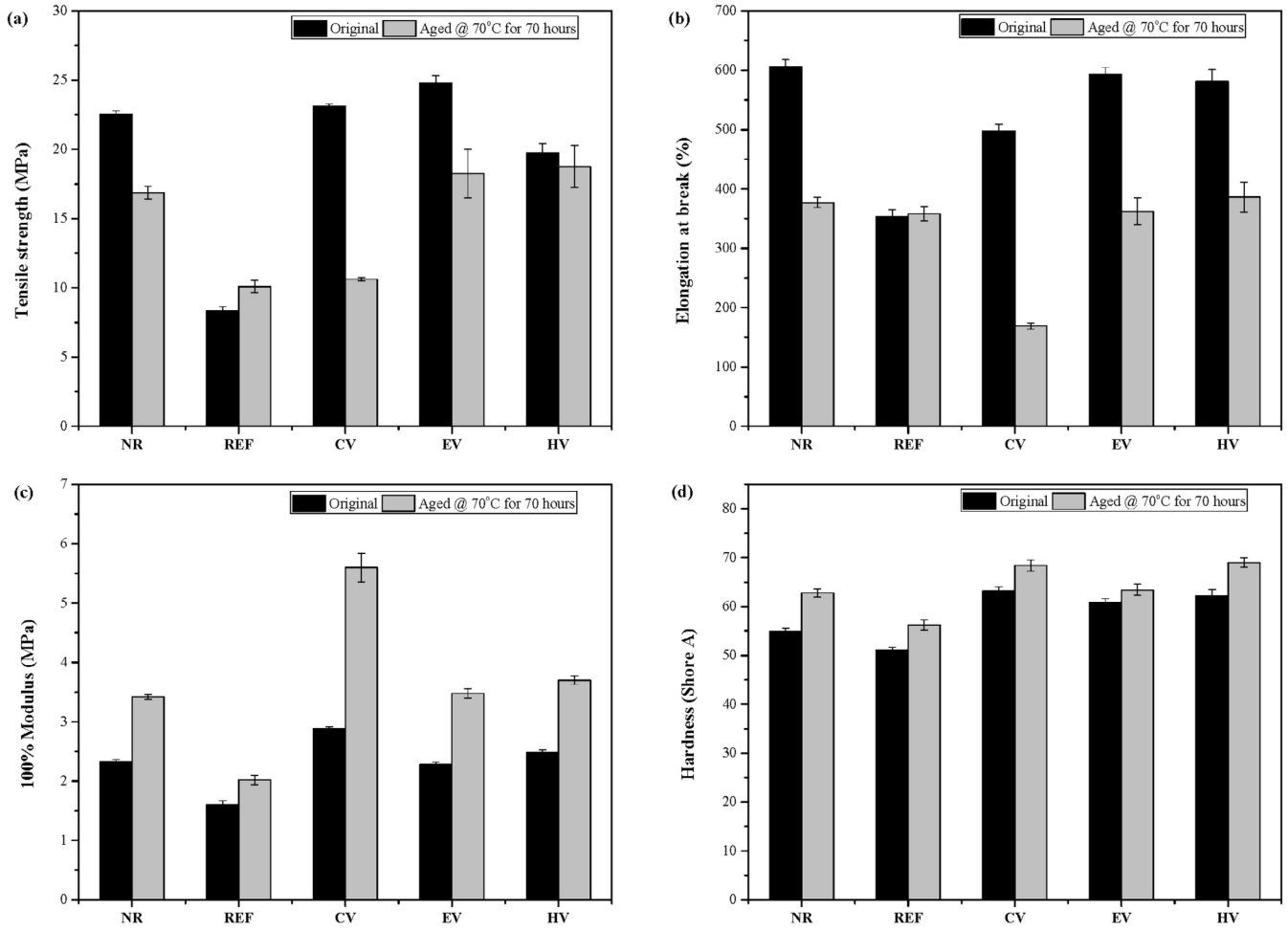

FIGURE 5 | Physical and mechanical properties of the Group-1 vulcanizates before and after aging (a) Tensile strength (b) Elongation at break (c) 100% tensile modulus, (d) Hardness.

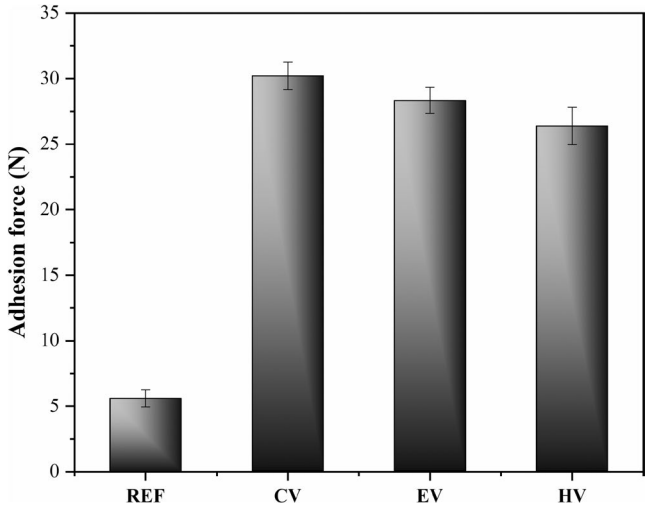

FIGURE 6 | Adhesion force values of the Group-1 vulcanizates.

were evaluated and compared. Dynamic strain and frequency sweep results were discussed in order to evaluate Payne effect and processability, respectively. Scanning electron microscopy (SEM) images were examined to correlate the topography with the overall material properties.

3.2.1 | Rheological and Mechanical Properties

The rheometer curves of ENR compounds, prepared with the coagent-induced cure system (HV) containing various amounts of amino silane-modified wollastonite (formulations provided in Table 1), are presented in Figure 8, alongside the reference NR and REF compounds. The key rheological parameters are summarized in Table 3. It was observed that with the increase in the wollastonite content, the maximum torque values increased, and the highest MH value was reached with the HV-20A compound. There was no significant change in the ML values, which are associated with the compound viscosity. However, it was observed that with the addition of wollastonite, the cure extent, i.e., the number of crosslinks, also increased. This is expected to affect the hardness and modulus values which will be discussed in a later section in this paper (Figure 8). There was no significant change in the scorch time with the increase in wollastonite content. However, the optimum cure time increased, which consequently led to a decrease in the cure rate index.

It is believed that the functional groups in the structure of wollastonite interact with accelerators, which play an active role in sulfur vulcanization, thereby reducing the concentration of free accelerators in the reaction environment. As a result, the

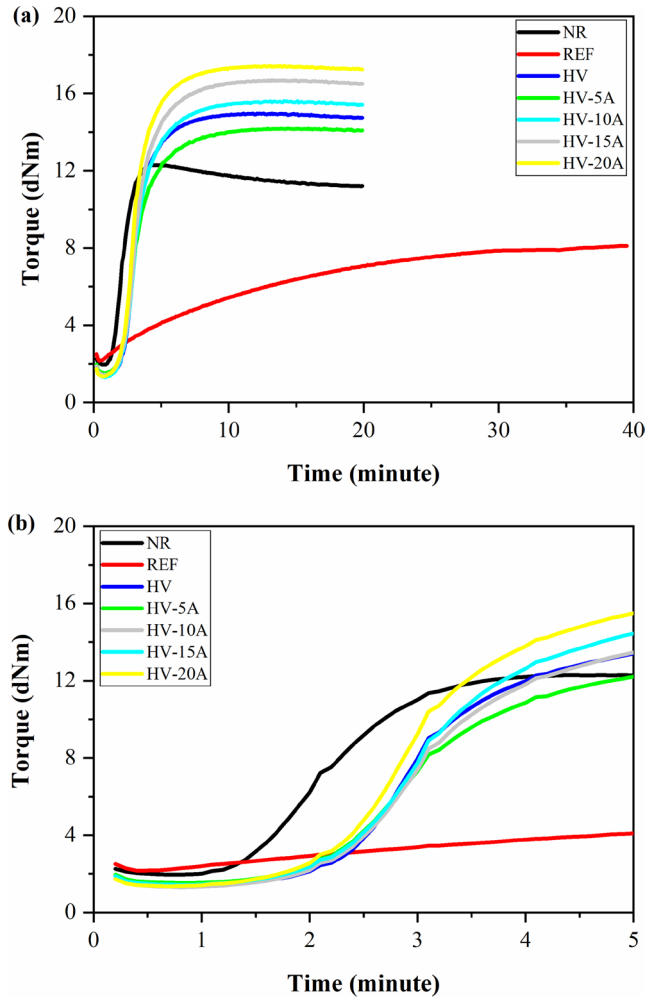

FIGURE 7 | Effect of wollastonite on cure characteristics: (a) Original rheometer curves, (b) Extended rheometer curves of the Group-2 compounds.

vulcanization process is expected to slow down. In the literature, it has been demonstrated that when the surfaces of fillers are modified with reactive silanes, the dispersion of the filler improves remarkably. However, this also exhibits an effect that slows down the vulcanization process [48–50]. In the study conducted by Ismail et al. [48] it was shown that the slower vulcanization observed in the compounds prepared by adding halloysite nanotubes (HNT) to ENR, particularly at high HNT concentrations, was due to the absorption of amine and alcohol groups as well as metallic ions from the accelerators by the silanol groups in the HNT structure. In another study, it was reported that the scorch time and optimum cure time of nanocomposites prepared by adding different amounts (0.5–2.5 phr) of multi-walled carbon nanotubes (MWCNT) to ENR-30, were increased. This effect was attributed to the absorption of accelerators by the carboxyl groups on the surface of the MWCNTs [50].

As can be seen from the rheometer curves (Figure 7), with the addition of wollastonite, a closer initial cure profile to that of the NR compound was obtained compared to the control compound prepared with the coagent-induced curing system (HV). This suggests that the designed inner liner formulations may exhibit higher adhesion to the NR compound, that was used as the base surface.

When the rheological data of Group-2 compounds given in Table 3 are examined, it is observed that the addition of wollastonite caused an increase in the cure extent. This is attributed to the amino reactivity on the silane-modified wollastonite, which promotes epoxy ring opening reaction in ENR, thereby forming additional covalent bonds. Studies in the literature also support this view, demonstrating that in the presence of reactive silanes, fillers undergo ring-opening reactions with the epoxy groups on the ENR main chain, further enhancing the formation of additional covalent bonds. Nakaramontri et al. [51] showed that the addition of 3-aminopropyltriethoxysilane (APTES) and bis (triethoxysilyl propyl) pentasulfide (TESPT) silane coupling agents to the ENR/carbon nanotube (CNT) matrix resulted in higher cure extent. Using Fourier Transform Infrared Spectroscopy (FTIR) and X-ray Photoelectron Spectroscopy (XPS), Charoeythornkhajhornchai et al. [52] showed that the $-NH_2$ functional group in the structure of amino silane-modified graphene oxide reacts with the epoxy groups on ENR, leading to the epoxy ring opening reaction. In another study, it was shown that amino silane-modified carbon nanotubes promote the ring-opening of ENR. This was explained by the increase in the intensity of the Si–O–Si and Si–O–C stretching vibration bands in FTIR spectrum [38].

As seen in Table 3, the Mooney viscosity increased with an increase in the wollastonite content, as indicated by the higher ML values. This is a common occurrence in rubber compounds when inorganic fillers are incorporated. Depending on their concentration, inorganic fillers can restrict chain mobility in the rubber matrix leading to an increase in viscosity. In the literature, numerous studies explain this phenomenon for both wollastonite and other inorganic fillers [27, 53–56]. However, as seen in the Group-2 compounds, the addition of relatively low amounts of wollastonite does not result in a significant or systematic change in the scorch times of the compounds. When higher amounts are used, it is observed that wollastonite acts like a vulcanising agent, accelerating the scorch time. Similar findings have previously been reported [25].

The tensile strength, elongation at break, 100% tensile modulus, hardness, and tear strength values of the Group-2 compounds are given in Figures 8 and 9. As it is seen from Figure 8, the initial tensile strength of the HV compound is 19.7 MPa, and this value gradually decreases with the addition of wollastonite. The interaction of wollastonite with the rubber matrix is lower compared to highly reinforcing fillers such as carbon black. This can also negatively impact filler dispersion due to low reinforcement and dispersion effects, hindering stress transfer between chains during tensile deformation, resulting in lower tensile strength [25, 28]. With the addition of wollastonite, the tensile modulus, i.e., rigidity of the material increased, leading to an increase in hardness, while the elongation at break values decreased. The increase in the modulus of the material is attributed to the hard and fibrous structure of wollastonite, which can lead to a decrease in material flexibility [29, 45]. Upon thermal aging, all vulcanizates showed a decrease in tensile strength and elongation at break, along with an increase in modulus and hardness due to oxidative stiffening. However, the wollastonite-filled samples retained their tensile strength and modulus better than the HV compound, in most instances. This finding indicates improved thermal stability and can be

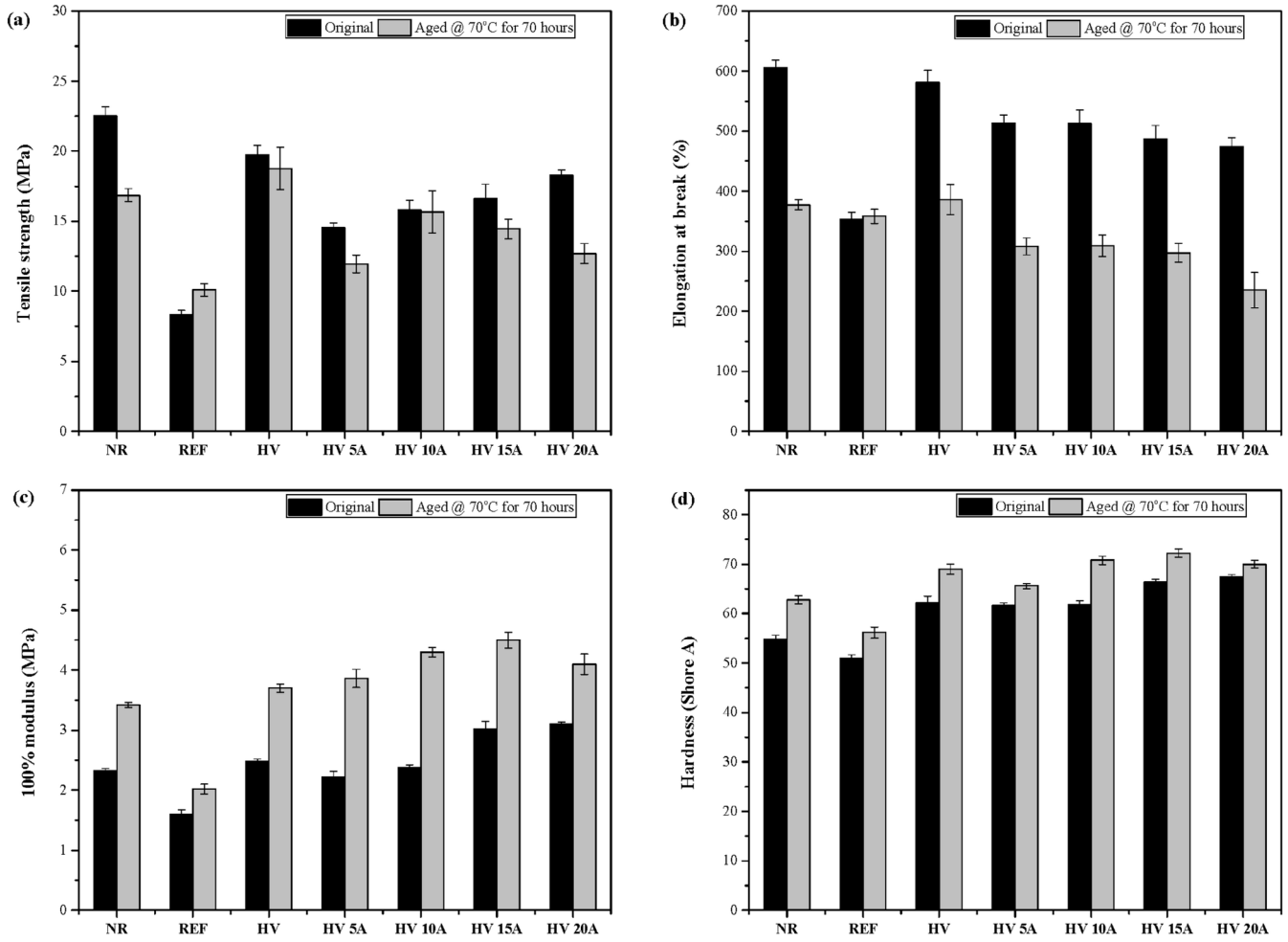

FIGURE 8 | Mechanical properties of the Group-2 vulcanizates before and after aging (a) tensile strength (b) elongation at break (c) 100% modulus (d) Hardness.

TABLE 3 | Rheological data of the Group-2 compounds.

	ML (dNm)	MH (dNm)	t_{s2} (min)	t_{90} (min)	CE (dNm)	CRI (min^{-1})
NR	2.8 ± 0.1	12.9 ± 0.2	1.7 ± 0.1	3.2 ± 0.1	10.2 ± 0.2	64.6 ± 2.4
REF	2.2 ± 0.1	8.2 ± 0.1	4.3 ± 0.1	25.8 ± 0.1	6.1 ± 0.1	4.7 ± 0.1
HV	1.3 ± 0.1	15.0 ± 0.1	2.3 ± 0.1	5.2 ± 0.1	13.7 ± 0.1	34.3 ± 1.1
HV-5A	1.5 ± 0.1	13.9 ± 0.4	2.4 ± 0.1	5.8 ± 0.1	12.4 ± 0.4	30.1 ± 1.6
HV-10A	1.3 ± 0.1	16.0 ± 0.4	2.3 ± 0.1	5.6 ± 0.1	14.7 ± 0.4	29.7 ± 1.1
HV-15A	1.4 ± 0.1	16.7 ± 0.3	2.4 ± 0.1	5.8 ± 0.1	15.3 ± 0.3	28.9 ± 0.4
HV-20A	1.4 ± 0.1	17.6 ± 0.2	2.3 ± 0.1	5.4 ± 0.1	16.2 ± 0.1	31.6 ± 1.0

attributed to the inorganic nature and thermal conduction performance of wollastonite, which enhances heat dissipation and limits oxidative degradation. The rigid filler also restricts chain mobility, contributing to network stabilization. Nonetheless, elongation at break decreased notably with higher filler content, showing that increased stiffness after aging was achieved at the expense of flexibility. In summary, wollastonite improved the thermal aging resistance in terms of strength and rigidity but reduced elasticity.

Figure 9 shows that all ENR compounds exhibit lower tear strength compared to the NR compound but higher than the butyl liner compound (REF). In the compounds where the wollastonite content exceeds 5 phr, tear strength is adversely affected. This result can be associated with the poor dispersion of the inorganic wollastonite in the rubber matrix [57, 58]. In addition, the incorporation of high amounts of inorganic fillers can create a large interfacial area within the rubber matrix, increasing stress leading to lower tear strength [59].

When examining the mechanical properties after aging, it was observed that epoxidised natural rubber has better thermal aging resistance than natural rubber but, as expected, was weaker compared to butyl rubber. Additionally, the presence of wollastonite in ENR compounds does not have a significant effect on aging. After aging, the property changes in NR and ENR show a decrease in tensile strength and elongation at break, while the 100% tensile modulus and hardness increase. These changes are as expected for rubbers with a polyisoprene structure [60, 61]. In butyl rubber, it was observed that the additional crosslinks formed during thermal aging increase the modulus and hardness, as well as the tensile strength and elongation at break. Consequently, butyl rubber is not adversely affected by thermal aging. It is expected that the aging mechanisms in rubber matrices will progress differently. During aging, chain scission and the formation of crosslinks occur simultaneously. A portion of the sulfur that did not participate in vulcanization can become activated during aging, leading to the formation of new crosslinks. These effects can result in different consequences depending on the rubber main chain structure [28, 29].

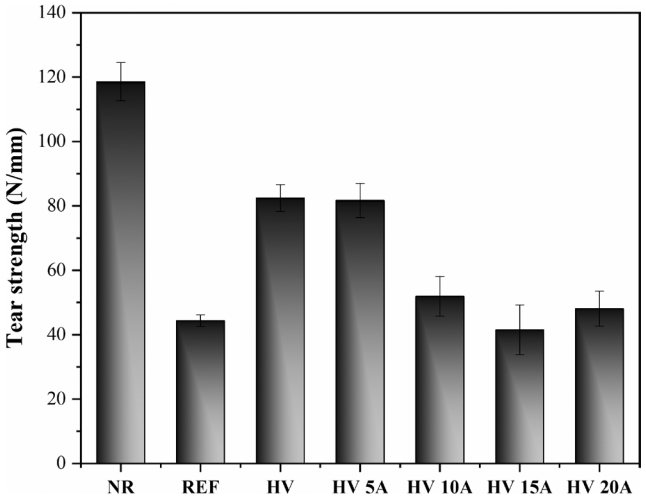

FIGURE 9 | Tear strength of the Group-2 vulcanizates.

3.2.2 | Dynamic Properties

In the multifaceted evaluation of the effect of fillers added to rubber compounds, the monitoring of their dynamic properties under increasing frequency and strain conditions is frequently utilized. The damping factor (tan δ) measured during the frequency sweep on the compound is proportional to the viscous component of the compound, and a high tan δ value can be associated with better processability. When examining the

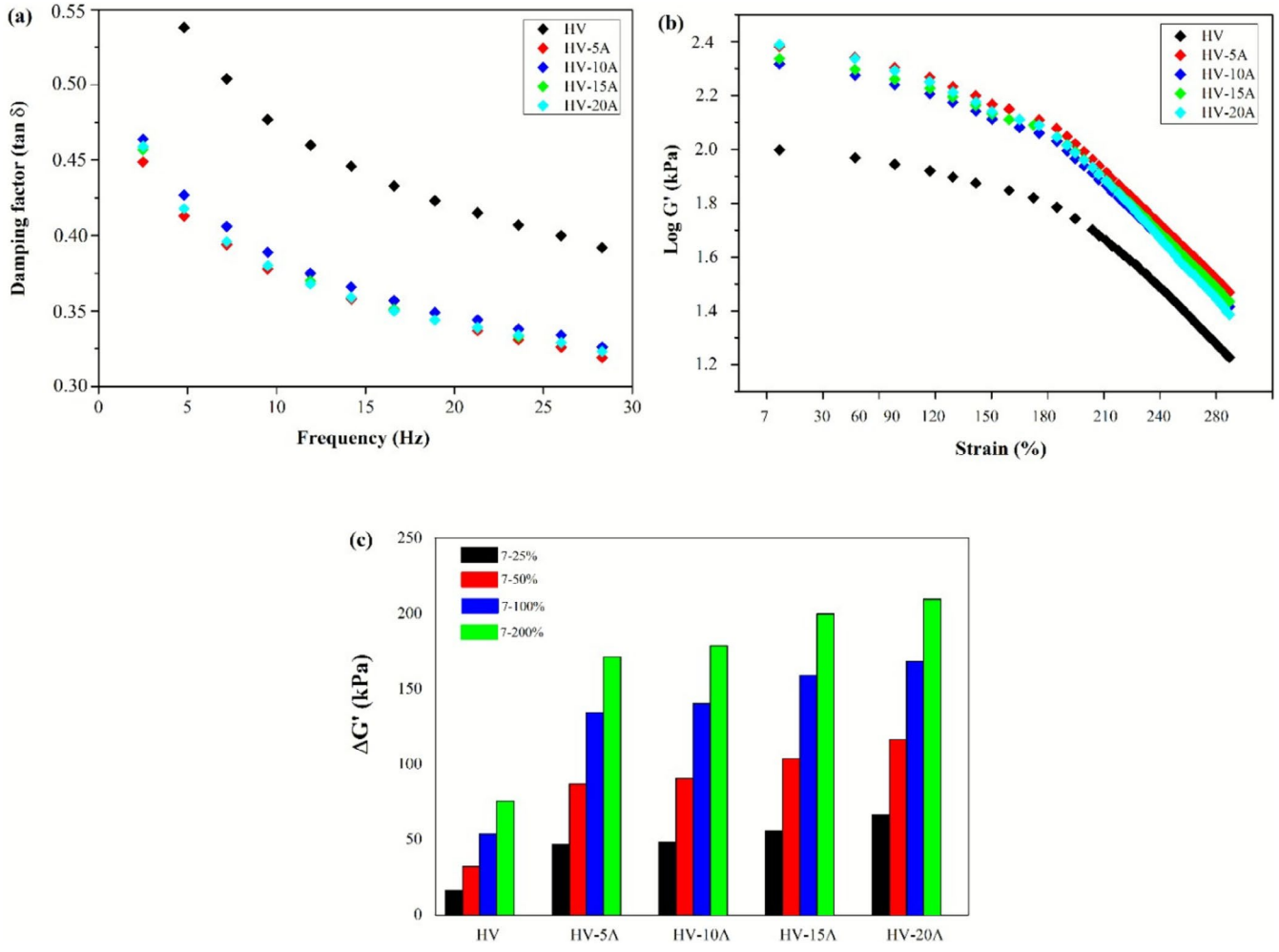

FIGURE 10 | (a) Tan δ values of the Group-2 compounds as a function of frequency, (b) Payne effect of the Group-2 compounds: Storage modulus for 7%–200% strain range, (c) Delta storage modulus ($\Delta G'$) for different strain ranges.

tan δ vs. frequency given in Figure 10a, it was observed that the highest tan δ values are measured in the HV compound, and tan δ decreased with the addition of wollastonite. The decrease in tan δ values with the addition of wollastonite, and consequently the lower processability, is an expected result for many fillers added to rubber compounds. Looking at the ML values on the rheometer curves, there is no significant change detected in viscosity with the addition of wollastonite. When these findings are evaluated collectively, it can be concluded that since the dynamic conditions during the compound preparation stage are closer to the rheometer test conditions, wollastonite is not expected to have a negative effect on processability during the compound preparation stage. However, at higher deformation rates, experienced during extrusion and injection, it may have a slightly negative impact on the processability. Since processes with low deformation rates, such as calendaring, are predominantly used in the shaping of tyre inner liner compounds, this impact is not expected to be a significant drawback in industrial applications.

The Payne effect is a method used to evaluate polymer-filler/additive interactions and dispersion efficiency. These interactions are related to changes in the rubber microstructure. The variation in strain-dependent storage modulus primarily provides insight into polymer-filler interactions in the high-strain region, while in the low-strain region, it reflects filler dispersion and filler-filler interactions. If the polymer-filler interaction is weak and/or the filler does not exhibit good dispersion, agglomeration is expected to occur. In this case, a significant loss in storage modulus is observed with the increasing strain levels under dynamic conditions. The difference between the storage moduli at low and high strain conditions is defined as the Payne effect. The lower the Payne effect, the better the interaction between the polymer and the filler. However, filler-filler interactions and polymer-filler interactions are usually opposing characteristics [62–65].

Figure 10b,c show the Payne effect and the levels of the Payne effect at different strain ranges, respectively. Upon examining Figure 10b, it was observed that the Payne effect increased with the increase in wollastonite content. The addition of wollastonite negatively impacted the homogeneity of the compound due to the difficulty it causes in adhesion to the rubber matrix. The decrease in compound homogeneity leads to agglomerate formation in the main matrix, which in turn results in weaker rubber-filler interactions. According to the Payne effect results at different strain ranges shown in Figure 10c, the HV compound was found to have a lower storage modulus difference compared to all other compounds with wollastonite addition, regardless of the strain range. Although there is nearly a 50% difference in the storage moduli between the HV compound and the other compounds at low strain values (7%–25% and 7%–50%), this difference was observed to be higher at higher strain values (7%–100% and 7%–200%). This is thought to be due to the lower rubber-filler interaction caused by the addition of wollastonite in the high strain ranges. As described in previous sections, this effect can be attributed to wollastonite not being a reinforcing filler. In the low-strain regions, the increase in wollastonite content does not show a significant change in the Payne effect, which suggests that there is a synergistic interaction between carbon black and wollastonite.

3.2.3 | Adhesion and Gas Barrier Properties

Figure 11a shows the adhesion strength values of Group-2 vulcanizates. The adhesion strength of the HV sample is 24.4 ± 1.43 N, approximately five times greater than that of the REF sample. However, when wollastonite was added to the HV compound, this improvement increased to eight times, irrespective of the amount added. This significant improvement is thought to be due to the ability of ENR to vulcanize alongside NR, as well as the rod-like structure of wollastonite, which supports physical bonding between the two rubber phases. It is believed that wollastonite exhibits a stitching effect, among the limited number of studies in the literature discussing the enhancement of adhesion by wollastonite in polymeric matrices, Chen et al. [66] reported that the addition of wollastonite to PP improved interfacial adhesion. In another study, it was found the addition of wollastonite to isotactic PP/Metallocene-catalyzed ethylene-propylene copolymer (EPR) blend improved the interfacial adhesion [67]. This study also presented the correlation between the interfacial adhesion strength and the thermodynamic work of adhesion values calculated through contact angle measurements.

We have shown the effect of wollastonite on adhesion for the first time in an ENR matrix, resulting in remarkably higher improvement in adhesion than the levels previously reported in the literature. When evaluated in terms of the amount of

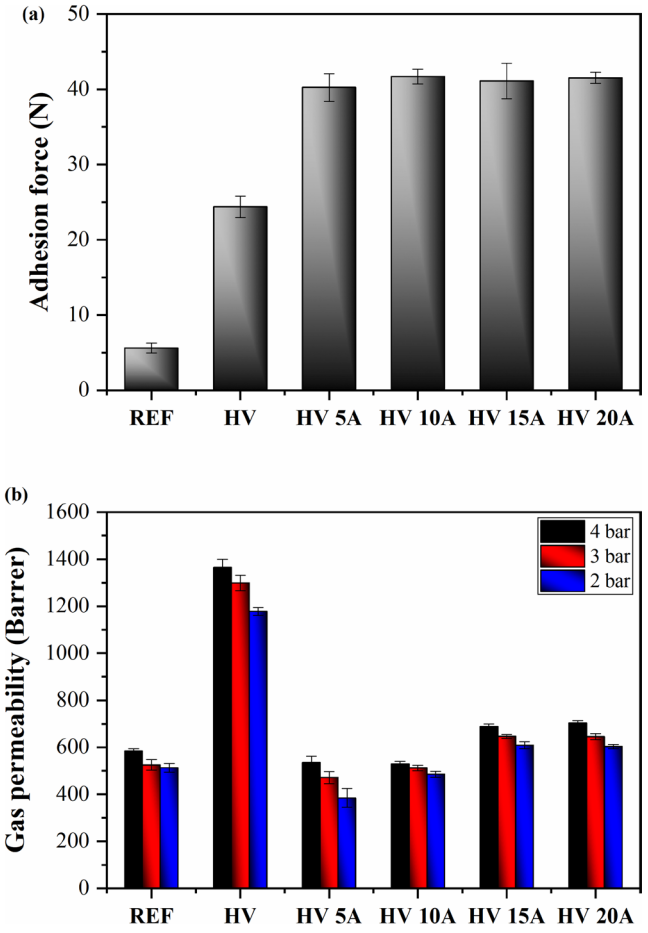

FIGURE 11 | (a) Adhesion force values (b) gas permeability of the Group-2 vulcanizates.

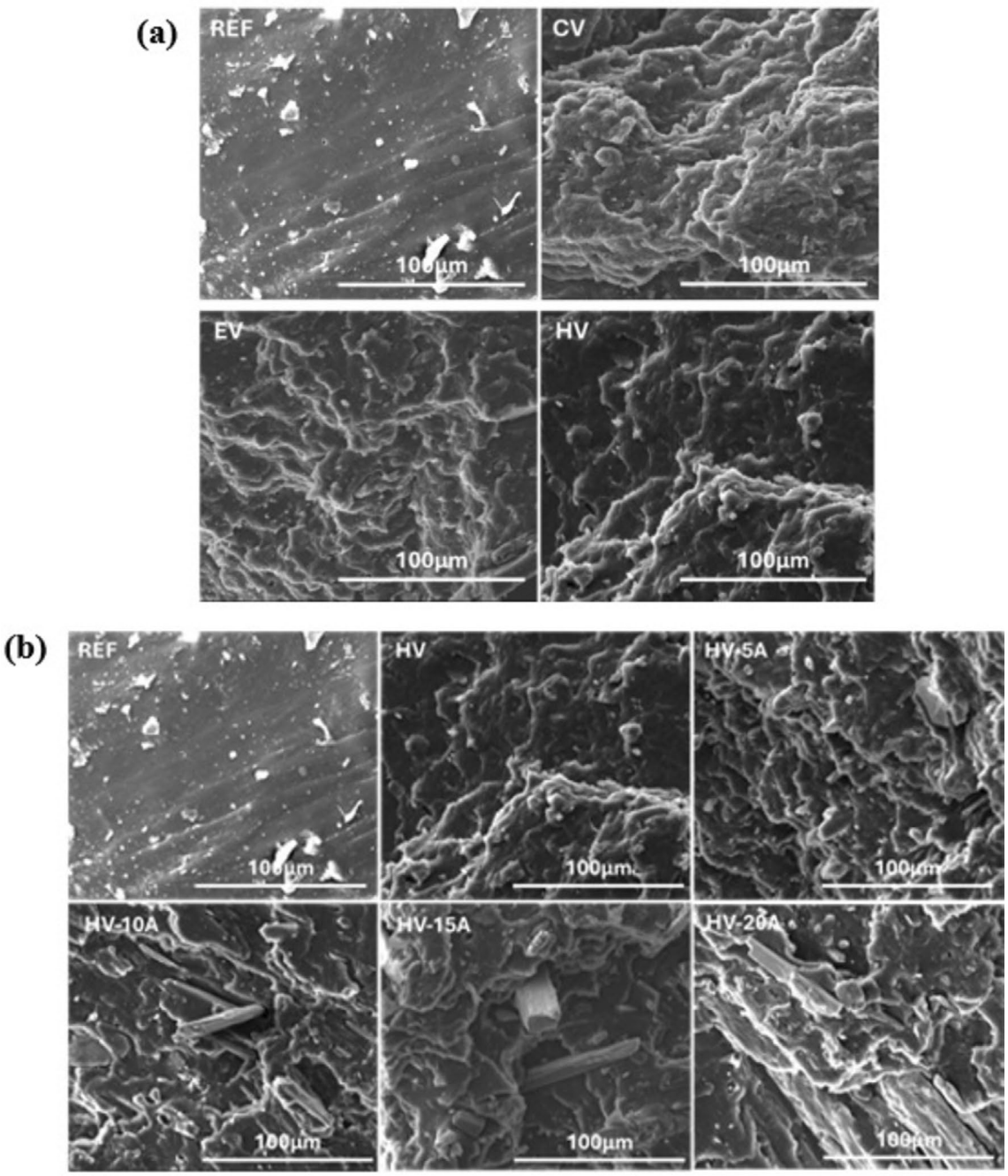

FIGURE 12 | SEM images of the (a) Group-1 vulcanizates (b) Group-2 vulcanizates.

wollastonite added to the ENR matrix, no systematic or significant change was observed. In the HV 5A vulcanizate, which contains 5 phr of wollastonite, the adhesion strength was 40.2 ± 1.84 N, while in the vulcanizate with the highest wollastonite content (20 phr), i.e., HV 20A, it was measured to be 41.5 ± 0.75 N.

Figure 11b presents the permeability results of the vulcanizates for dry air, measured at different pressure differentials. Butyl rubber is known as the synthetic rubber with the lowest gas permeability, therefore the highest gas barrier properties [68–70]. When examining Figure 11b, as expected, the butyl rubber-based REF vulcanizate provides much lower permeability, offering a barrier effect approximately 2 times greater than the ENR-based HV vulcanizate, due to its well-known lower permeability compared to many other rubber matrices. However, it was also observed that with the addition of wollastonite, the gas permeability was reduced to a level very close to that of butyl rubber. It is understood that fillers increase the tortuous path within the polymeric matrix, thereby reducing gas permeability by hindering gas passage [71–73]. The addition of wollastonite makes the gas passage path more tortuous, reducing the permeability value and thereby enhancing the material's gas barrier performance. In the case of low wollastonite addition (5 phr), a lower gas permeability than butyl rubber was measured, that is attributed to relatively good dispersion of the filler in the rubber matrix. In fact, in the HV 5A compound, the gas barrier property was significantly improved at 2 bar, which is closer to the

pressure of air typically pumped into tyres during application, compared to butyl rubber.

The fundamental objective of this study was to design a tyre inner liner compound that can approach the gas barrier properties of butyl rubber whilst exhibiting higher adhesion to the NR-based carcass compound, thereby improving the final performance of the tyre. In addition, we aimed to evaluate the effect of wollastonite on improving the gas barrier properties of ENR. In all compounds containing wollastonite from the Group-2, not only was the obtained adhesion strength up to eight times greater than that of butyl rubber, but also the gas permeability was lower than that of butyl rubber. The HV 5A compound, which contains 5 phr of wollastonite and prepared using a coagent-induced vulcanization system, is therefore considered to offer significant advantages as a tyre inner liner compound compared to of butyl rubber.

3.2.4 | Topographical Analysis

SEM images of the rubber samples in both groups of vulcanizates revealed distinct topographical features depending on their chemical composition. Butyl rubber-based REF sample exhibited the smoothest surface (Figure 12a), which may explain the low tear resistance and poor adhesion force associated with this sample. This smooth microstructure likely results in poor physical interaction within polymer matrices. While the CV, EV, and HV samples exhibited similar surface features and textures, they also demonstrated comparable mechanical properties as shown in Figure 12a.

Among Group 1 compounds, HV was selected to investigate the influence of wollastonite ratio on the properties of Group-2 compounds. Figure 12b displays the topographical differences between Group-2 compounds and the REF sample, which exhibits a distinctly smooth surface and a dense structure. As previously shown (Figure 11b), the REF sample demonstrated superior gas barrier properties compared to HV, not due to its dense topography but rather its chemical structure, i.e., a butyl rubber-based vulcanizate. In wollastonite-containing HV samples, the interaction between amino silane and epoxy is expected to enhance gas diffusion properties. Notably, incorporating 5 phr of wollastonite led to a significant improvement in gas barrier performance, even surpassing that of the REF sample. However, beyond this concentration, the barrier properties began to decline. This initial enhancement is attributed to increased tortuosity, which forces gas molecules to navigate more complex diffusion pathways. However, as the wollastonite content increases further, the introduction of voids and poorer dispersion will likely create additional pathways for gas diffusion due to its high aspect ratio, systematically reducing the overall gas barrier performance.

4 | Conclusions

This study aimed to develop an epoxidised NR-based compound as an alternative to butyl rubber for tyre inner liners, offering enhanced gas barrier properties and improved adhesion to other tyre rubber compounds. To achieve this, wollastonite, a natural mineral filler with a high aspect ratio, was incorporated into the ENR formulation. The ENR compounds were divided into two groups for evaluation. The first group focused on identifying the optimal curing system that could achieve curing behavior comparable to the NR-based compound while ensuring strong adhesion between the liner and carcass. Bismaleimide-induced vulcanization was found to provide the best balance of scorch safety, which is critical for a liner compound, along with adequate mechanical properties and thermal stability. The second group was formulated using this curing system with varying amounts of wollastonite to enhance interfacial adhesion and reduce gas permeability. The effect of wollastonite on adhesion was evaluated in an ENR matrix for the first time, achieving a significantly greater improvement than previously reported in literature. The addition of just 5 phr of amino silane-modified wollastonite resulted in an eightfold increase in adhesion strength, surpassing that of butyl rubber. This remarkable enhancement was attributed to the rod-like structure of wollastonite, which increases the complexity of the gas diffusion path by introducing greater tortuosity. In conclusion, this study demonstrates that an ENR-based compound reinforced with wollastonite presents a highly promising alternative to butyl rubber for tyre inner liners, offering superior adhesion and enhanced gas barrier properties.

Author Contributions

T.Ü.Y. conducted a significant portion of the experimental work and prepared the initial draft of the manuscript. A.E. contributed to the experimental work. R.J. participated in the interpretation of the experimental results and the writing of the manuscript. B.K. conceived the study concept, designed the experimental steps and the overall structure of the manuscript, and performed the initial editing. C.S. contributed to the evaluation of the experimental data and to the final editing of the manuscript.

Acknowledgments

This study was funded by The Scientific and Technological Research Council of Türkiye (Project no: 123M175) and by Kocaeli University BAP Department (Project no: FOA-2023-3167). The authors gratefully thank for their valuable support.

Funding

This work was supported by Türkiye Bilimsel ve Teknolojik Araştırma Kurumu, 123M175 and Kocaeli University BAP Department, FOA-2023-3167.

Disclosure

The manuscript was written through contributions of all authors. All authors have given approval to the final version of the manuscript. For the purpose of open access, the author has applied a Creative Commons Attribution (CC BY) license to any Author Accepted Manuscript version of this paper, arising from this submission.

Conflicts of Interest

The authors declare no conflicts of interest.

Data Availability Statement

The data that support the findings of this study are available from the corresponding author upon reasonable request.

References

1. A. T. Raju, B. Dash, P. Dey, S. Nair, and K. Naskar, "Evaluation of Air Permeability Characteristics on the Hybridization of Carbon Black With Graphene Nanoplatelets in Bromobutyl Rubber/Epoxidized Natural Rubber Composites for Inner-Liner Applications," *Polymers for Advanced Technologies* 31 (2020): 2390–2402.

2. S. A. H. Mohammad, J. Timar, and J. Walker, "Inner Liner for Use in a Tubeless Pneumatic Tire," 1984, European Patent Office EP 0102844A2.

3. K. F. Lin and D. W. Klosiewicz, "Tire Innerliner," 1991, United States Patent US5040583A.

4. L. L. D. Colantonio, A. T. Peronnet-Paquin, F. G. Corvasce, A. E. F. Roesgen, and F. Philpott, "Self-Supporting Pneumatic Tire With a Partial Inner Liner," 2006, United States Patent US 6988522B2.

5. B. Karaağaç, D. Kaner, and V. Deniz, "The Effects of Compatibility on the Mechanical Properties and Fatigue Resistance of Butyl/EPDM Rubber Blends," *Polymer Composites* 31, no. 11 (2010): 1869–1873.

6. K. Formela and J. T. Haponiuk, "Curing Characteristics, Mechanical Properties and Morphology of Butyl Rubber Filled With Ground Tire Rubber (GTR)," *Iranian Polymer Journal* 23, no. 3 (2014): 185–194.

7. Y. Han, H. Zheng, Y. Liu, et al., "Synergistic Development of Natural Rubber/Butyl Rubber Composites for Improved Interfacial Bonding and Enhanced Shock-Absorbing Capabilities," *ACS Omega* 9, no. 12 (2024): 13897–13905.

8. K. Sankaran, P. Manoharan, S. Chattopadhyay, et al., "Effect of Hybridization of Organoclay With Carbon Black on the Transport, Mechanical, and Adhesion Properties of Nanocomposites Based on Bromobutyl/Epoxidized Natural Rubber Blends," *RSC Advances* 6, no. 40 (2016): 33723–33732.

9. T. R. Aswathy, B. Dash, P. Dey, S. Nair, and K. Naskar, "Synergistic Effect of Graphene With Graphene Oxide, Nanoclay, and Nanosilica in Enhancing the Mechanical and Barrier Properties of Bromobutyl Rubber/Epoxidized Natural Rubber Composites," *Journal of Applied Polymer Science* 138, no. 31 (2021): 50746, https://doi.org/10.1002/app.50746.

10. M. A. Rahman, M. Penco, I. Peroni, G. Ramorino, A. M. Grande, and L. D. Landro, "Self-Repairing Systems Based on Ionomers and Epoxidized Natural Rubber Blends," *ACS Applied Materials & Interfaces* 3, no. 12 (2011): 4865–4874.

11. C. Jiang, H. He, X. Yao, P. Yu, L. Zhou, and D. Jia, "Self-Crosslinkable Lignin/Epoxidized Natural Rubber Composites," *Journal of Applied Polymer Science* 131, no. 23 (2014): 41166, https://doi.org/10.1002/app.41166.

12. F. A. Tanjung, A. Hassan, and M. Hasan, "Use of Epoxidized Natural Rubber as a Toughening Agent in Plastics," *Journal of Applied Polymer Science* 132, no. 29 (2015): 1–9.

13. L. Mascia, J. Clarke, K. S. Ng, K. S. Chua, and P. Russo, "Cure Efficiency of Dodecyl Succinic Anhydride as a Cross-Linking Agent for Elastomer Blends Based on Epoxidized Natural Rubber," *Journal of Applied Polymer Science* 132, no. 6 (2015): 41448, https://doi.org/10.1002/app.41448.

14. H. Ismail, "Potential of Rubberwood as a Filler in Epoxidized Natural Rubber Compounds," *Journal of Elastomers and Plastics* 33, no. 1 (2001): 34–46.

15. R. A. Al-Mansob, A. Ismail, A. N. Alduri, C. H. Azhari, M. R. Karim, and N. I. M. Yusoff, "Physical and Rheological Properties of Epoxidized Natural Rubber Modified Bitumens," *Construction and Building Materials* 63 (2014): 242–248.

16. C. M. Vu, H. T. Vu, and H. J. Choi, "Fabrication of Natural Rubber/Epoxidized Natural Rubber/Nanosilica Nanocomposites and Their Physical Characteristics," *Macromolecular Research* 23, no. 3 (2015): 284–290.

17. X. Zhao, K. Niu, Y. Xu, et al., "Morphology and Performance of NR/NBR/ENR Ternary Rubber Composites," *Composites Part B: Engineering* 107 (2016): 106–112.

18. A. Krainoi, C. Kummerlöwe, Y. Nakaramontri, et al., "Influence of Critical Carbon Nanotube Loading on Mechanical and Electrical Properties of Epoxidized Natural Rubber Nanocomposites," *Polymer Testing* 66 (2018): 122–136.

19. A. Arefi Pour, S. Sharifnia, R. NeishaboriSalehi, and M. Ghodrati, "Performance Evaluation of Clinoptilolite and 13X Zeolites in CO_2 Separation From CO_2/CH_4 Mixture," *Journal of Natural Gas Science and Engineering* 26 (2015): 1246–1253.

20. A. J. Montes Luna, G. Castruita de León, S. P. García Rodríguez, N. C. Fuentes López, O. Pérez Camacho, and Y. A. Perera Mercado, "Na^+/Ca^{2+} Aqueous Ion Exchange in Natural Clinoptilolite Zeolite for Polymer-Zeolite Composite Membranes Production and Their $CH_4/CO_2/N_2$ Separation Performance," *Journal of Natural Gas Science and Engineering* 54 (2018): 47–53.

21. S. Haner and D. Çuhadaroğlu, "Wollastonite: A Review," *Geology Engineering Journal* 37, no. 1 (2013): 63–82.

22. H. G. Karian, *Handbook of Polypropylene and Polypropylene Composites*, 2nd ed. (Marcel Dekker, 2003).

23. J. U. Zilles, *Wollastonites. Fillers for Polymer Applications*, ed. R. Rothon (Springer International Publishing, 2017).

24. E. Park, "Mechanical Properties and Processibility of Glass-Fiber-Wollastonite, and Fluoro-Rubber-Reinforced Silicone Rubber Composites," *Journal of Applied Polymer Science* 105, no. 2 (2006): 460–468.

25. H. T. B. Diep, H. Ismail, A. R. Azura, N. Van Tu, and T. Takeichi, "The Effect of Wollastonite on Curing Characteristics, Tensile and Morphology of Natural Rubber Compounds," *Advanced Materials Research* 858, no. 2013 (2013): 199–204.

26. I. Yuhaida, H. Salmah, I. Hanafi, and Z. Firuz, "The Effect of Acrylic Acid on Tensile and Morphology Properties of Wollastonite Filled High Density Polyethylene/Natural Rubber Composites," *Procedia Chemistry* 19 (2016): 401–405.

27. P. S. Khobragade, J. B. Naik, and A. Chatterjee, "Polystyrene-Grafted Wollastonite Nanofiller for Styrene Butadiene Rubber Nanocomposite: Rheological, Thermal and Mechanical Studies," *Polymer Bulletin* 74, no. 5 (2016): 1915–1934.

28. Y. Xiao, L. Yan, T. Chang, et al., "Preparation of High-Quality Wollastonite/Natural Rubber Composites by Atomization Sputtering Rapid Drying Process," *Polymer Bulletin* 80 (2022): 6263–6284.

29. Y. Xiao, Y. Hao, L. Yan, et al., "Mechanism on Surface Hydrophobically Modification of Fibrous Wollastonite and Its Reinforcement of Natural Rubber," *Journal of Polymer Research* 29 (2022): 342, https://doi.org/10.1007/s10965-022-03194-0.

30. A. Chatterjee, P. S. Khobragade, and S. Mishra, "Physicomechanical Properties of Wollastonite ($CaSiO_3$)/styrene Butadiene Rubber (SBR) Nanocomposites," *Journal of Applied Polymer Science* 132, no. 47 (2015): 42811, https://doi.org/10.1002/app.42811.

31. N. Akçakale and Ş. Bülbül, "The Effect of Mica Powder and Wollastonite Fillings on the Mechanical Properties of NR/SBR Type Elastomer Compounds," *Journal of Rubber Research* 20, no. 3 (2017): 157–167.

32. K. Berry, M. Liu, K. Chakraborty, et al., "Mechanism for Cross-Linking Polychloroprene With Ethylene Thiourea and Zinc Oxide," *Rubber Chemistry and Technology* 88, no. 1 (2015): 80–97, https://doi.org/10.5254/rct.14.85986.

33. L. Virág, A. Egedy, C. Varga, et al., "Determination of the Most Significant Rubber Components Influencing the Hardness of Natural Rubber (NR) Using Various Statistical Methods," *Heliyon* 10, no. 3 (2024): e25170, https://doi.org/10.1016/j.heliyon.2024.e25170.

34. K. Ghosal and B. N. Freeman, "Gas Separation Using Polymer Membranes: An Overview," *Polymers for Advanced Technologies* 5, no. 11 (1994): 673–697.

35. F. U. Nigiz, "Synthesis and Characterization of Grapheme Nanoplate-Incorporated PVA Mixed Matrix Membrane for Improved Separation of CO_2," *Polymer Bulletin* 77 (2020): 2405–2422.

36. F. U. Nigiz and N. D. Hilmioğlu, "Enhanced Hydrogen Purification by Grapheme-Poly(Dimethyl Siloxane) Membrane," *International Journal of Hydrogen Energy* 45 (2020): 3549–3557.

37. T. Ünügül and F. U. Nigiz, "Hydrogen Purification Using Natural Zeolite-Loaded Hydroxyethyl Cellulose Membrane," *International Journal of Energy Research* 46, no. 2 (2022): 1826–1836.

38. A. M. Shanmugharaj and S. H. Ryu, "Influence of Aminosilane-Functionalized Carbon Nanotubes on the Rheometric, Mechanical, Electrical and Thermal Degradation Properties of Epoxidized Natural Rubber Nanocomposites," *Polymer International* 62, no. 10 (2013): 1433–1441.

39. N. Hayeemasae, K. Waesateh, S. Saiwari, H. Ismail, and N. Othman, "Detailed Investigation of the Reinforcing Efect of Halloysite Nanotubes-Filled Epoxidized Natural Rubber," *Polymer Bulletin* 78 (2021): 7147–7166.

40. B. N. Yeşil, T. Ünügül, and B. Karaağaç, "Self-Healing Behaviour of Lignin-Containing Epoxidized Natural Rubber Compounds," *Express Polymer Letters* 17, no. 7 (2023): 704–721.

41. N. Rattanason, A. Poonsuk, and T. Makmoon, "Effect of Curing System on the Mechanical Properties and Heat Aging Resistance of Natural Rubber/Tire Tread Reclaimed Rubber Blends," *Polymer Testing* 24 (2005): 728–732.

42. N. H. H. Shuhaimi, N. S. Ishak, N. Othman, H. Ismail, and S. Sasidharan, "Effect of Different Types of Vulcanization Systems on the Mechanical Properties of Natural Rubber Vulcanizates in the Presence of Oil Palm Leaves-Based Antioxidant," *Journal of Elastomers & Plastics* 46, no. 8 (2014): 747–764.

43. S. Rabiei and A. Shojaei, "Vulcanization Kinetics and Reversion Behavior of Natural Rubber/Styrene-Butadiene Rubber Blend Filled With Nanodiamond—The Role of Sulfur Curing System," *European Polymer Journal* 81 (2016): 96–113.

44. R. C. Tomazi, N. B. Guerra, M. Glovanela, S. Moresco, and J. S. Crespo, "Evaluation of Vulcanization Systems in Natural Rubber Elastomeric Tire Sidewall Compositions With Lignin as a Stabilizing Agent," *Polymer Bulletin* 70 (2023): 8977–8994.

45. H. Ismail, U. S. Ishiaku, A. R. Arinab, and Z. A. Mohd-Ishak, "Epoxidized Natural Rubber Compounds: Effect of Vulcanization Systems and Fillers," *Polymer-Plastics Technology and Engineering* 37, no. 4 (1998): 469–481.

46. Z. A. Mohd-Ishak, P. Y. Wan, P. L. Wong, Z. Ahmad, U. S. Ishıaku, and J. Karger-Kocsis, "Effects of Hygrothermally Decomposed Polyurethane on the Curing and Mechanical Properties of Carbon Black-Filled Epoxidized Natural Rubber Vulcanizates," *Journal of Applied Polymer Science* 84, no. 12 (2002): 2265–2276.

47. Z. Cai, D. Cadek, M. Jindrova, A. Kaderabkova, and A. Kuta, "Physical Properties and Biodegradability Evaluation of Vulcanized Epoxidized Natural Rubber/Thermoplastic Potato Starch Blends," *Materials* 15, no. 21 (2022): 7478, https://doi.org/10.3390/ma15217478.

48. H. Ismail and R. Nordin, "Effect of Epoxidized Natural Rubber (ENR) and Ethylene-Co-Acrylic Acid Copolymer on Properties of Silica-Filled Natural Rubber/Recycle Rubber Powder Blends," *Polymer-Plastics Technology and Engineering* 43, no. 2 (2004): 285–300.

49. H. Ismail, S. Z. Salleh, and Z. Ahmad, "Properties of Halloysite Nanotube (HNT) Filled SMR L and ENR 50 Nanocomposites," *International Journal of Polymeric Materials and Polymeric Biomaterials* 62, no. 6 (2013): 314–322.

50. S. Chuayjuljit, P. Mungmeechai, and A. Boonmahitthisud, "Mechanical Properties, Thermal Behaviors and Oil Resistance of Epoxidized Natural Rubber/Multiwalled Carbon Nanotube Nanocomposites Prepared via In Situ Epoxidation," *Journal of Elastomers and Plastics* 49, no. 2 (2016): 99–119.

51. Y. Nakaramontri, C. Nakason, C. Kummerlöwe, and N. Vennemann, "Effects of In-Situ Functionalization of Carbon Nanotubes With Bis(Triethoxysilylpropyl) Tetrasulfide (TESPT) and 3-Aminopropyltriethoxysilane (APTES) on Properties of Epoxidized Natural Rubber–Carbon Nanotube Composites," *Polymer Engineering and Science* 55 (2015): 2500–2510.

52. P. Charoeythornkhajhornchai and A. Somwangthanaroj, "Synthesis of Graphene Oxide Grafted With Epoxidized Natural Rubber via Aminosilane Linkage," *Materials Science Forum* 940 (2018): 28–34.

53. A. Sanchez-Arroyo, M. Rodriguez-Reyes, B. O. Villarreal-Fuentes, et al., "Combined Effect of TiO_2 and Metallurgical Slag Addition on the Properties of Magnesium Composites," *Journal of Materials Engineering and Performance* 34 (2024): 18844–18857, https://doi.org/10.1007/s11665-024-10585-5.

54. N. Phuhiangpa, W. Ponloa, S. Phongphanphanee, and W. Smitthipong, "Performance of Nano- and Microcalcium Carbonate in Uncrosslinked Natural Rubber Composites: New Results of Structure–Properties Relationship," *Polymers* 12, no. 9 (2020): 1–15.

55. E. Ojogbo, C. Tzoganakis, and T. H. Mekonnen, "Batch Mixing for the In Situ Grafting of Epoxidized Rubber Onto Cellulose Nanocrystals," *ACS Sustainable Chemistry & Engineering* 10 (2022): 8743–8753.

56. A. S. Sethulekshmi, J. S. Jayan, A. Saritha, and K. Joseph, "Recent Developments in Natural Rubber Nanocomposites Containing Graphene Derivatives and Its Hybrids," *Industrial Crops and Products* 177 (2022): 114529, https://doi.org/10.1016/j.indcrop.2022.114529.

57. M. Bhattacharya, S. Biswas, S. Bandyopadhyay, and A. K. Bhowmick, "Influence of the Nanofiller Type and Content on Permeation Characteristics of Multifunctional NR Nanocomposites and Their Modeling," *Polymers for Advanced Technologies* 23 (2012): 596–610.

58. W. Intiya, U. Thepsuwan, C. Sirisinha, and P. Sae-Oui, "Possible Use of Sludge Ash as Filler in Natural Rubber," *Journal of Material Cycles and Waste Management* 19 (2017): 774–781.

59. P. Intharapat, A. Kongnoo, and K. Kateungngan, "The Potential of Chicken Eggshell Waste as a Bio-Filler Filled Epoxidized Natural Rubber (ENR) Composite and Its Properties," *Journal of Polymers and the Environment* 21 (2013): 245–258.

60. N. M. Mathew and S. K. De, "Thermo-Oxidative Ageing and Its Effect on the Network Structure and Fracture Mode of Natural Rubber Vulcanizates," *Polymer* 24, no. 8 (1983): 1042–1054.

61. X. Zhang, T. Lin, Z. Tang, B. Guo, and G. China, "Elastomeric Composites Based on Zinc Diacrylate-Cured Epoxidized Natural Rubber: Mechanical Properties and Ageing-Resistance," *Elastomers and Plastics* 7, no. 8 (2015): 39–45.

62. J. Ramier, C. Gauthier, L. Chazeau, L. Stelandre, and L. Guy, "Payne Effect in Silica-Filled Styrene–Butadiene Rubber: Influence of Surface Treatment," *Journal of Polymer Science Part B: Polymer Physics* 45 (2006): 286–298.

63. F. Zhao, X. Shi, X. Chen, and S. Zhao, "Interaction of Vulcanization and Reinforcement of CB on Dynamic Property of NR Characterized by RPA2000," *Journal of Applied Polymer Science* 117, no. 2 (2010): 1168–1172.

64. J. Wu, L. Chen, B. L. Su, and Y. S. Wang, "Evolution of Payne Efect of Silica-Filled Natural Rubber in Curing Process," *Journal of Rubber Research* 22 (2019): 127–132.

65. T. Ünügül and B. Karaağaç, "Vulcanization of Chlorinated Polyethylene/Chloroprene Rubber Compounds at Lower Temperatures in the Presence of Reactive Silanes," *Journal of Applied Polymer Science* 138, no. 23 (2021): 50544, https://doi.org/10.1002/app.50544.

66. M. Chen, C. Wan, W. Shou, Y. Zhang, Y. Zhang, and J. Zhang, "Effects of Interfacial Adhesion on Properties of Polypropylene/Wollastonite Composites," *Journal of Applied Polymer Science* 107, no. 3 (2008): 1718–1723.

67. I. Svab, V. Musil, A. Pustak, and I. Smit, "Wollastonite-Reinforced Polypropylene Composites Modified With Novel Metallocene EPR Copolymers. II. Mechanical Properties and Adhesion," *Polymer Composites* 30, no. 8 (2008): 1091–1097.

68. G. J. van Amerongen, "Diffusion in Elastomers," *Rubber Chemistry and Technology* 37, no. 5 (1964): 1065–1152.

69. R. H. Boyd and P. V. Krishna Pant, "Molecular Packing and Diffusion in Polyisobutylene," *Macromolecules* 24 (1991): 6325–6331.

70. F. Cai, G. You, X. Zhao, H. Hu, and S. Wu, "The Relationship Between Specific Structure and Gas Permeability of Bromobutyl Rubber: A Combination of Experiments and Molecular Simulations," *Macromolecular Theory and Simulations* 28, no. 6 (2019): 1900025, https://doi.org/10.1002/mats.201900025.

71. X. Yuan, A. J. Easteal, and D. Bhattacharyya, "Influence of Surface Treatment on Hybrid Wollastonite-Polyethylene Composite Resins for Rotational Moulding," *Journal of Materials Science* 43 (2008): 6057–6063.

72. X. Yang, Y. Zhang, Y. Xu, S. Gao, and S. Guo, "Effect of Octadecylamine Modified Graphene on Thermal Stability, Mechanical Properties and Gas Barrier Properties of Brominated Butyl Rubber," *Macromolecular Research* 25, no. 3 (2017): 270–275.

73. A. Dutta, J. Chanda, T. Bhandary, et al., "Influence of Organically Modified Clays on the Barrier Properties of Bromo Butyl Rubber Composites for Tyre Inner Liner Application," *Polymer-Plastics Technology and Materials* 61, no. 18 (2022): 2049–2062.